New Journal of Physics
The open access journal at the forefront of physics

Deutsche Physikalische Gesellschaft DPG | IOP Institute of Physics

Antihydrogen trapping assisted by sympathetically cooled positrons

N Madsen[1], **F Robicheaux**[2] **and S Jonsell**[3]
[1] Department of Physics, Swansea University, Swansea, SA2 8PP, UK
[2] Department of Physics, Purdue University, West Lafayette, IN 47097, USA
[3] Department of Physics, Stockholm University, SE-10691 Stockholm, Sweden
E-mail: N.Madsen@swan.ac.uk

Received 11 February 2014, revised 23 April 2014
Accepted for publication 13 May 2014
Published 19 June 2014
New Journal of Physics **16** (2014) 063046
doi:10.1088/1367-2630/16/6/063046

Abstract
Antihydrogen, the bound state of an antiproton and a positron, is of interest for use in precision tests of nature's fundamental symmetries. Antihydrogen formed by carefully merging cold plasmas of positrons and antiprotons has recently been trapped in magnetic traps. The efficiency of trapping is strongly dependent on the temperature of the nascent antihydrogen, which, to be trapped, must have a kinetic energy less than the trap depth of $\sim$0.5 K k_B. In the conditions in the ALPHA experiment, the antihydrogen temperature seems dominated by the temperature of the positron plasma used for the synthesis. Cold positrons are therefore of paramount interest in that experiment. In this paper, we propose an alternative route to make ultra-cold positrons for enhanced antihydrogen trapping. We investigate theoretically how to extend previously successful sympathetic cooling of positrons by laser-cooled positive ions to be used for antihydrogen trapping. Using simulations, we investigate the effectiveness of such cooling in conditions similar to those in ALPHA, and discuss how the formation process and the nascent antihydrogen may be influenced by the presence of positive ions. We argue that this technique is a viable alternative to methods such as evaporative and adiabatic cooling, and may overcome limitations faced by these. Ultra-cold positrons, once available, may also be of interest for a range of other applications.

Keywords: non-neutral plasma, antihydrogen, particle transport, sympathetic cooling

1. Introduction

Antihydrogen, the bound state of an antiproton and a positron, holds the promise of unprecedented precision in the study of matter–antimatter symmetry in nature. The recent successful trapping of antihydrogen ($\bar{\mathrm{H}}$) [1–3] means that we can expect the first precision spectroscopy of a pure antimatter system shortly, and that detailed comparisons of the energy levels or gravitational responses of antihydrogen and hydrogen may soon be carried out. The first steps in both directions have already been carried out by the ALPHA collaboration [4, 5]. While the long time confinement demonstrated in [2] was important to the positron spin-flip experiment [4], more sensitive comparisons likely require both more than one antiatom trapped at a given time and colder antiatoms than are currently available. It is thus of great interest to study methods by which the trapping efficiency can be enhanced, colder antihydrogen may be formed, and by which antihydrogen could be cooled as recently proposed [6].

The standard schemes in use for making trappable antihydrogen make use of two opposing wells in a Penning–Malmberg trap to hold cold plasmas of positrons $\left(\mathrm{e}^{+}\right)$ and antiprotons ($\bar{\mathrm{p}}$) respectively, and then either rely on an autoresonant drive to change the antiproton axial energy such that they come into contact with the positrons [1, 7] or on slowly merging the plasmas through potential manipulations [3]. The Penning–Malmberg traps used in all of these experiments use a strong axial magnetic field for the transverse confinement of the charged particles and individually excitable co-axial cylindrical electrodes to provide axial electric fields for axial confinement. The traps are kept at cryogenic temperatures of 2–7 K. Leptons trapped in the strong magnetic field will emit cyclotron radiation and approach thermal equilibrium with their surroundings, whose effective temperature may however be dominated by indirect sources such as acoustic or electronic noise. In earlier antihydrogen experiments using merged plasmas it was found that the antihydrogen created was not in thermal equilibrium with the cold positrons [8]. This was found to be due to the fact that the antiprotons were launched into the positrons with several eV of relative energy. In the autoresonance-based scheme used by ALPHA for successful trapping, the antihydrogen seems to be formed at or close to the temperature of the positron plasma, i.e. the antiprotons reach thermal equilibrium with the positron plasma before forming antihydrogen [2]. This is consistent with calculated equilibration rates of ~200 Hz for typical experimental parameters in ALPHA [9]. This implies that to make colder antihydrogen, and thus increase the trapping efficiency in the ALPHA scheme, the positron temperature needs to be lowered.

The positron temperature in any such experiment will be influenced by the radiation temperature and noise temperature of the surroundings. Controlling these parameters imposes constraints on the construction of the apparatus (i.e. cryogenics, electronic noise, etc) and on the ease of access for other purposes, such as lasers for spectroscopy. A further influential factor is the strong non-homogeneous magnetic fields needed for the antihydrogen trap. These magnetic fields can have a strong disturbing influence on the non-neutral plasmas used for antihydrogen formation [10, 11]. Additional, active cooling, may combat these various heating sources, and potentially make the positrons colder than the surroundings. Two such methods have been demonstrated to work for large numbers of particles in plasmas composed of electrons $\left(e^{-}\right)$, positrons or antiprotons. The first was evaporative cooling, routinely used for atoms, which was used in the ALPHA trapping experiments to both cool positrons and antiprotons [1, 12]. The second, is the technique of adiabatic cooling by expansion, which has been demonstrated on antiprotons [13]. Both of these methods have achieved cryogenic temperatures of 3–10 K. However, there are several limitations when these methods are used for antihydrogen trapping. The first is that positrons are strongly interacting with the surroundings through their cyclotron motion, and constant efficient cooling is needed to maintain low temperatures. This is difficult, if not impossible, to achieve with either of the two methods. The second is that both methods cause the plasma to expand, evaporative cooling causing radial expansion, and adiabatic cooling causing a lengthening. Larger plasmas are more susceptible to the inhomogeneous magnetic fields used for the atom trap [12]. This again leads to the need for constant efficient cooling.

Here we theoretically investigate an alternative route to cold positrons for antihydrogen using sympathetically cooled e^+. Sympathetic laser-cooling is a well established technique used for cooling ions, atoms or molecules that do not lend themselves to direct cooling methods [14–16]. Using laser-cooled $^9Be^+$, sympathetic cooling of a small number of positrons was demonstrated by Jelencovic *et al* in 2002 but not pursued any further [17, 18]. In their experiment Jelenkovic *et al* cooled and compressed a few thousand positrons to less than 5 K using $\sim 10^6$ $^9Be^+$ ions in a room-temperature Penning–Malmberg trap. We propose to extend these initial experiments to cool the millions of positrons used in current antihydrogen trapping experiments. A number of questions are addressed to investigate the feasibility of this method to enhance the formation of cold, trappable antihydrogen. The two main questions are if (a) it is possible to effectively cool a large quantity of positrons by using laser-cooled positive ions and (b) how will the presence of the positive ions influence the formation, trapping and survival of antihydrogen. We find that with a careful choice of parameters and particle numbers it is possible to achieve temperatures that are about an order of magnitude lower than the currently best documented positron plasma temperatures [2]. We also find that it is important to use as light a cooling ion as possible, making the $^9Be^+$ ions used in the original proof-of-principle experiments the best choice. We furthermore find that the dominant influence of the positive ions on antihydrogen trapping is antiproton capture by the positive ion. However, with typical numbers of cooling ions at about 10% of the number of positrons, the combination of centrifugal separation of the ions and positrons and the injection of antiprotons predominantly on axis reduce the influence of this process to negligible levels.

2. Antihydrogen formation and trapping using autoresonance

Antihydrogen for trapping may be formed by merging cold plasmas of $\bar{p}$'s and e^+s. Experiments by ATHENA determined early on that the traditional $\bar{H}$ synthesis technique that launched eV $\bar{p}$'s into a cold e^+ plasma, generated $\bar{H}$ that was too energetic to be trapped [8]. ALPHA first attempted to solve this issue by merging the plasmas by slowly moving the potentials holding the $\bar{p}$'s and e^+s in neighbouring wells [19]. The technique did not result in trapped $\bar{H}$ in ALPHA, but a similar technique was reported to result in trapped $\bar{H}$ in the ATRAP experiment [3]. ALPHA instead employs a novel technique using autoresonance [20, 21] to excite the $\bar{p}$'s collectively in their well until they enter the e^+ plasma [7]. This technique makes use of the fact

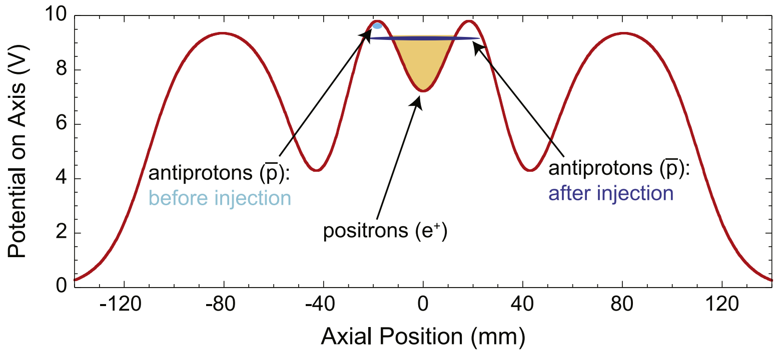

Figure 1. The electrical potentials used by the ALPHA experiment for merging cold $\bar{p}$'s and e^+ to make cold $\bar{H}$ [1].

that an anharmonic oscillator will lock to an external drive under certain conditions and, by carefully chirping the drive frequency, energy can be transferred to the oscillator in a deterministic fashion. As the contact between the drive and the particles is destroyed at the moment the antiprotons enter the positron plasma this allows for minimal relative axial energy difference between the two species on injection [22]. To trap $\bar{H}$, ALPHA prepares the $\bar{p}$'s and e^+s in neighbouring wells, energizes the magnetic trap (see below), evaporatively cools the e^+s and finally merges the two by autoresonantly exciting the $\bar{p}$'s into contact with the e^+s (see figure 1).

Neutral atoms may be trapped by acting on their intrinsic magnetic moment, that arises mainly due to the e^- spin (e^+ spin for antiatoms). The potential energy of an atom with magnetic moment $\vec{\mu}$ in a magnetic field $\vec{B}$ is given by

$$U = -\vec{\mu} \cdot \vec{B}. \tag{1}$$

The atoms may thus be trapped in a minimum in magnetic field strength in three dimensions. Such a setup allows capture of atoms with magnetic moments antiparallel to the magnetic field, also called low-field seekers. A magnetic minimum can be created by introducing two axially separated co-axial coils and a co-axial transverse multipole. As there are no readily available methods to cool $\bar{H}$ a key to trapping is that the antiatoms must be formed in the neutral trap.

The ALPHA experiment typically uses 2×10^6 positrons at about 40 K that are merged with 30 000 antiprotons by autoresonant injection of the latter [1]. The positrons form a cold plasma with radius 0.9 mm and a density of 5×10^7 cm^{-3}. The injected antiproton cloud has a radius of 0.4 mm at ~100 K. These typical parameters will be used in the following as a starting point for our calculations. With these parameters the ALPHA team typically traps about one antihydrogen atom for each experiment cycle of ~20 min [2].

3. Laser-cooling of ions

Only a limited number of ions are available for laser cooling as they must have a suitable level structure. We will focus on the two lightest ones that are readably coolable and constitute the work-horses of many activities in the field [23]. The positive magnesium ion $^{24}Mg^+$ has a convenient cooling transition at 279 nm from $3\,s^2S_{1/2} \rightarrow 3p^2P_{3/2}$, and the added advantage of isospin zero and thus no splitting due to nuclear spin. Magnesium is however almost three times more massive than $^9Be^+$ that has the same cooling transition at 313 nm, but the added complexity of a non-zero nuclear spin. Due to its simplicity for laser-cooling $^{24}Mg^+$ would be convenient, but we perform most calculations with the lighter $^9Be^+$ as mass differences play a critical role for the sympathetic cooling.

The minimum temperature attainable in a simple Doppler cooling-scheme where the laser is scattered on an ion considered to have just two levels is given by an equilibrium between the light force in the direction of the laser and the diffusive heating from the spatially symmetric spontaneous emission. This minimum temperature is called the Doppler limit and is given by [24]

$$T_D = \frac{\hbar \Gamma}{2k_B}, \tag{2}$$

where $2\pi\hbar$ is Planck's constant, Γ is the spontaneous decay rate and k_B is Boltzmann's constant. The value of this limit for Be^+ and Mg^+ is respectively 0.47 mK and 1.0 mK. As we will show below, such low temperatures appear to be a detriment so we do not plan to cool to mK temperatures.

The cooling power of the laser for typical laser-powers is in the tens of mW range and is in general large relative to typical heating sources, as is well documented by the low temperatures attainable in beam cooling experiments. In such experiments, laser-cooling has been shown to overcome the heating stemming from the large centre of mass energy of the beam [25]. In this study we therefore simplify our approach by assuming that laser-cooling can maintain the ions at any temperature that is much larger than T_D.

4. Multi-species non-neutral plasmas

A non-neutral plasma at equilibrium in a Penning trap will rotate around the axis of the trap due to the crossed magnetic and electric fields [26]. If the plasma is composed of more than one species (here defined as having different mass) the equilibrium distribution will be influenced by the difference in their so-called centrifugal potentials such that heavier species will tend to higher radii relative to lighter ones [26]. The temperature dependent separation of the two species was used by Jelenkovic *et al* on mixed $^9Be^+$ ions and e^+s to put an upper limit to the unmeasured temperature of the e^+s [18].

When the two species separate, the number of inter-species collisions will drop, thus the cooling power of the sympathetic cooling can be substantially diminished. In order to first investigate the separation, we have used a Poisson solver to find the equilibrium density of ions and e^+s for parameters of relevance to antihydrogen formation. We use a mixed plasma with 2×10^6 e^+s and 10^5 ions placed in the central potential well shown in figure 1. A temperature was set for both species and the resulting self-consistent density distribution was numerically calculated by relaxation using the same code as in [27]. Figure 2 shows the calculated radial density distribution for mixtures with Be^+ and Mg^+ at two different temperatures.

The increased separation of e^+s and ions with ion mass is clearly visible in the results in figure 2. It is highlighted by colouring the regions with non-zero density of both species. At e.g.

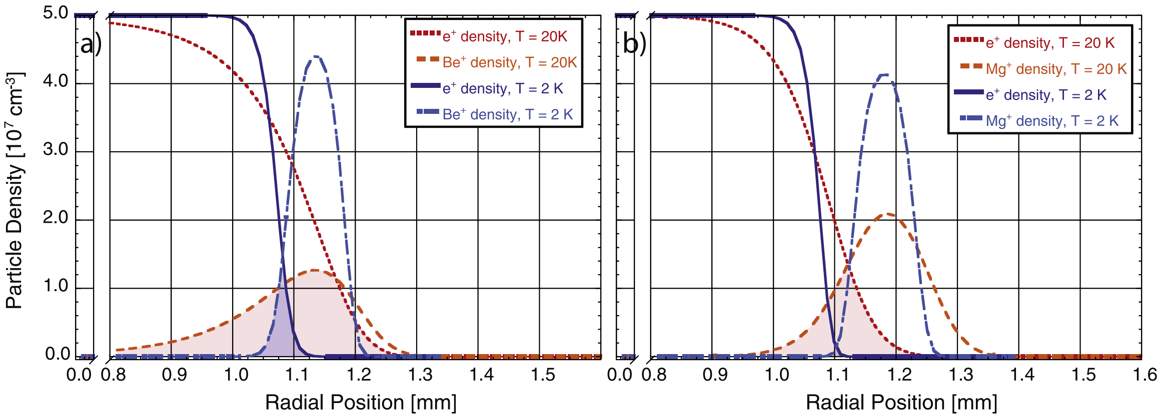

Figure 2. Equilibrium radial profiles calculated for (a) $^9Be^+$ ions and e^+ and (b) $^{24}Mg^+$ ions and e^+ and at 20 K and 2 K. The blue (red) shaded area indicates where the two 2 K (20 K) densities are simultaneously non-zero. Each calculation used two million e^+ and 10^5 ions in the ALPHA standard mixing potential (figure 1).

$T = 2$ K we see almost total separation of Mg^+ and e^+, whereas some overlap remains for Be^+ and e^+. Reduced overlap will lead to fewer inter-species collisions which may lead to reduced sympathetic cooling power for $^{24}Mg^+$ relative to $^9Be^+$.

5. Simulations of sympathetic cooling

Extending the code above to calculate the equilibrium temperature of the e^+ plasma with an imposed ion temperature, we can estimate how efficiently we can cool the e^+s using the two types of ions. From the simple physical overlap results above we expect that the lower contact at low temperatures between heavier ions and e^+ will lead to less cooling. We calculate the equilibrium temperature of the e^+s using collisions with the ions that are kept at fixed temperature, cyclotron cooling assuming a 7 K blackbody radiation environment as reported by ALPHA and finally we impose an additional heating rate $\left((\mathrm{d}T_e/\mathrm{d}t)_{\mathrm{ext}} \right)$ to simulate the observed heating of e^+s in the ALPHA experiment. The collision rate (Γ_{coll}) is proportional to the overlap of the densities of the two species, inversely proportional to the ion mass due to the dependence of the recoil on mass, and also approximately proportional to $T_e^{-3/2}$. The additional heating $\left((\mathrm{d}T_e/\mathrm{d}t)_{\mathrm{ext}} \right)$ is thought to stem from one or more sources comprising (a) internal surfaces that are not at 7 K, (b) leakage of external 300 K radiation into the positron region, (c) electronic noise on the electrodes used for the Penning–Malmberg trap and (d) heating due to particle motion in the inhomogeneous magnetic fields (see e.g. [28]). We use add-on heating rates in the range 26–52 K s^{-1} as taken from unreported experimental observations in ALPHA. We have not included plasma–plasma collective interactions in our code. Such interactions would likely lead to increased coupling between the positrons and the ions and therefore stronger sympathetic cooling. We will therefore consider our results as conservative estimates of what can be achieved. The equilibrium temperature is thus calculated by solving the following equation

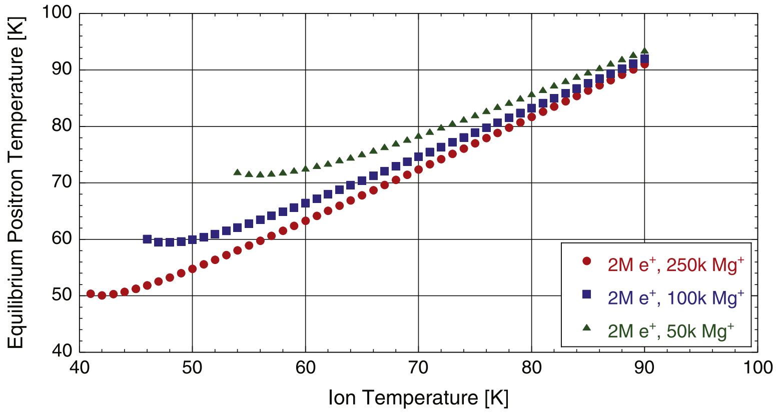

Figure 3. Calculated equilibrium temperature of 2×10^6 e^+s as a function of the Mg^+ temperature for three different quantities of cooling ions. The assumed external heating rate of the e^+s was 26 K s^{-1}, and the e^+ plasma radius was set to 0.81 mm. For ion temperatures below the points shown the e^+ temperature increases strongly.

using the self-consistent densities

$$\frac{dT_e}{dt} = \left(\frac{dT_e}{dt}\right)_{\text{ext}} - \left(T_e - T_{\text{rad}}\right) \times \Gamma_{\text{rad}} - \left(T_e - T_{\text{ion}}\right) \times \Gamma_{\text{coll}}, \tag{3}$$

where we keep T_{ion} fixed in these calculations. N_e and N_{ion} is respectively the number of positrons and ions. T_{rad} is the temperature of the walls (7 K) and Γ_{rad}^{-1} is the cyclotron cooling time (transverse to the magnetic field) given by

$$\Gamma_{\text{rad}}^{-1} = \frac{3\pi\epsilon_0 m_e c^3}{e^2\omega_c^2}, \tag{4}$$

as calculated from the classical Larmor formula, where ϵ_0 is the permittivity of free space, m_e the mass of the e^+, c the speed of light, e the charge of the positron and ω_c the cyclotron frequency. For the standard 1 T field in ALPHA this computes to 2.57 s.

Figure 3 shows the equilibrium temperature of two million e^+s mixed with three different quantities of Mg^+ ions as a function of the imposed ion temperature. Three trends stand out. First, the e^+ equilibrium temperature follows the ion temperature at higher ion temperature. Second, below some ion temperature, that depends on the number of ions, the e^+ temperature reaches a minimum. As the third trend we observe that the minimum temperature depends on the number of ions, such that an increase of the number of ions lead to a lower minimum temperature.

These trends follow the physics discussed previously. A higher ion number results in more collisions and thus more cooling power and therefore colder e^+s. As the temperature drops, the ions separate radially from the e^+s and the cooling power drops leading to a minimum achievable temperature. From the trend in figure 3 we can see that, we will need many more Mg^+ ions to achieve e^+ temperatures that are significantly better than those reported in [2].

In figure 4 we investigate how the minimum temperature depends on our choice of cooling ion and the number of ions. We indicate the error on the minimum temperature as the difference

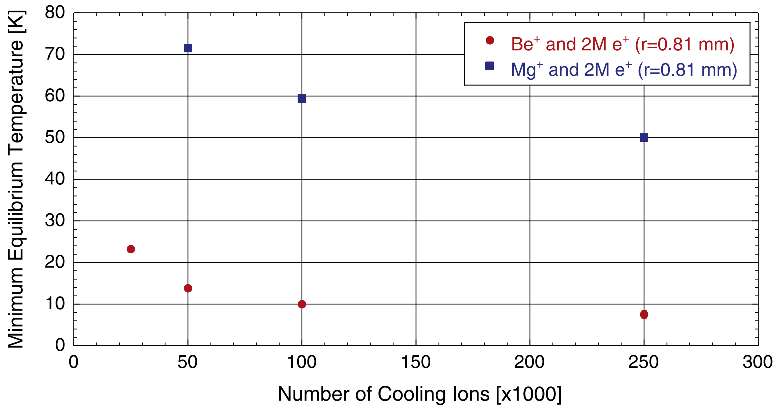

Figure 4. Calculated minimum temperature of 2×10^6 e^+s sympathetically cooled as a function of the number and type of ion. The assumed external heating rate of the e^+s was 26 K s^{-1} with Mg^+ and 52 K s^{-1} with Be^+. The e^+ plasma radius was 0.81 mm resulting in a peak density of 9.1×10^7 cm^{-3}.

to the nearest higher value. In some cases the simulation breaks down for the smallest temperatures and we estimate the error and the minimum using a trend-line. The most striking feature on figure 4 is the five fold drop in the minimum temperature caused by using Be^+ ions rather than Mg^+ ions even though the heating rate has been doubled for the Be^+ ions. This clearly makes Be^+ the preferred candidate for sympathetic cooling of e^+s. We also observe that while a larger number of ions initially results in more cooling, i.e. lower minimum temperature, this trend eventually saturates. This is consistent with the ions adding more and more layers on the outside of the multi-species plasma where additional ions only contribute in a limited way to the sympathetic cooling of the e^+s in the centre.

The separation of the two species as well as collision rates vary with the density. Experimentally the density is controlled by varying the size of the plasma and keeping the numbers constant. Figure 5 shows the minimum temperature for Be^+ cooled e^+s for three different e^+ plasma radii. The nominal radius in current experiments is 1 mm. Lower densities result in lower temperatures, in agreement with calculated larger overlap of the species at lower densities (figure 6). While this suggests continuously lowering the density, lower density may also result in lower antihydrogen formation rates [29], and larger plasmas could also be exposed to additional heating caused the inhomogeneous magnetic fields [19, 30]. Both these effects are beyond the scope of the studies here but will play a role for experimental investigations. The minimum e^+ temperature observed is around 5 K, about an order of magnitude lower than the 40 K observed in current ALPHA trapping experiments.

The heating rates used in these simulations are estimates based on observed behaviour in the ALPHA experiment and may of course be improved upon by better thermal shielding and lower electronic noise. However, the ultimate limit will be the heating caused by the large inhomogeneities in magnetic field imposed by the magnetic minimum trap for the neutral antihydrogen. In order to have an impression of how strongly the minimum temperature depends on the heating rate we have calculated the minimum temperature for a range of heating rates as shown in figure 7.

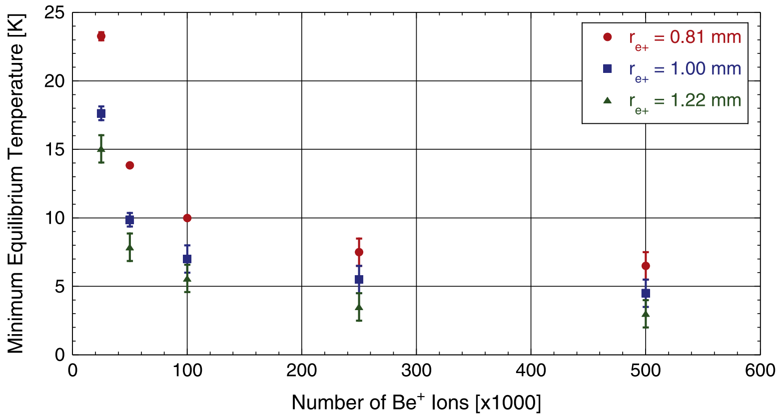

Figure 5. Calculated minimum temperature of 2×10^6 e^+s sympathetically cooled as a function of the number Be^+ ions and e^+ plasma radius. The radii 0.81 mm, 1.00 mm and 1.22 mm correspond to peak densities of 9.1, 6.2 and 4.3×10^7 cm^{-3} respectively. The assumed external heating rate of the e^+s was $52\ K\ s^{-1}$, independent of radius.

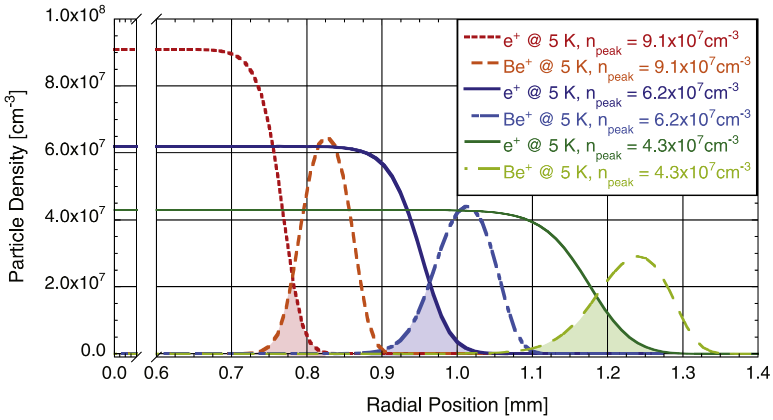

Figure 6. Equilibrium density distribution of 2×10^6 e^+ and 10^5 Be^+ for three different peak e^+ densities at $T_e = T_{\text{ion}} = 5$ K. The shaded colour indicates regions where the species overlap (both with non-zero density).

The calculated minimum of ∼5 K is therefore likely to improve in practice, as shielding is improved in the ongoing upgrade of the ALPHA apparatus [31]. However, if we conservatively assume that the improvement will be from 40 K to 5 K, and that, as reported in [2], the trap simply captures atoms with energies below threshold, the trapping rate should conservatively improve by a factor of ∼23. This improvement was estimated from integrating a Maxwellian distribution, assuming that the trap depth is much smaller than the width of the distribution, which gives a scaling of the trapped fraction with $T_{\bar{H}}^{-3/2}$. For 5 K $\bar{H}$ the well is still significantly shallower (∼$0.5\ K \cdot k_B$) than the width of the energy distribution. The trapping fraction scales as $T_e^{-3/2}$ under these circumstances. Other effects may improve on this rate, such as the increase in formation rate with lower temperatures, but estimating their effect on the trapping rate is rather involved and beyond the scope of this work.

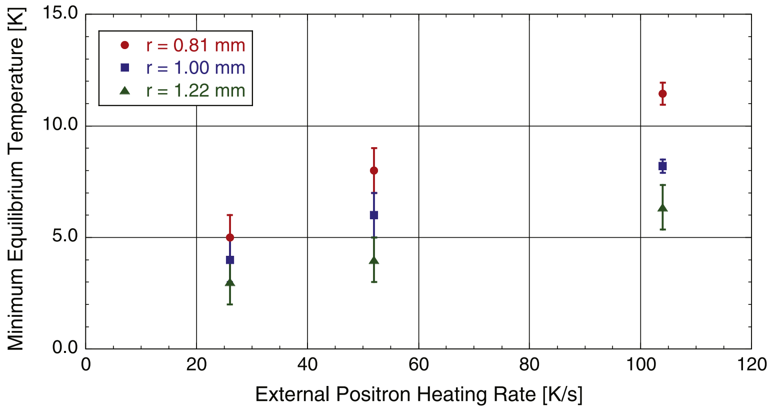

Figure 7. Calculated minimum temperature of 2×10^6 e^+s sympathetically cooled with 250 k Be^+ ions as a function of the imposed external heating rate of the e^+s.

We furthermore note that our calculations do not take collective effects into account, only single particle effects are included. Collective effects are likely to increase the coupling between the ion and the e^+ plasma which will serve to increase the cooling power and hence lower the minimum temperature. The results presented here may therefore be seen as a worst-case scenario.

If lower e^+ temperatures are desired, one may envisage further use of other details of antihydrogen formation. As an example, we note that about 90% of the antihydrogen atoms that are trapped in ALPHA seem to be formed during the first 100 ms of $e^+/\bar{p}$ mixing. If the cooling rate of the positron plasma, starting at e.g. 100 K is faster than the rate at which the species separate radially, the positrons may cool to lower temperatures than the equilibrium temperatures found here for a sufficiently long time to assist in antihydrogen trapping. The model we have employed in this work is too crude to say either way but it could be well worth investigating experimentally if the equilibrium temperatures turn out not to be as low as desired. In particular it's worth noting that the timescales for the centrifugal separation observed with mixtures of electrons and antiprotons are in the 100 ms range [27], thus comparable to the timescale on which antihydrogen is formed.

Two further limitations to ultra-low temperatures may be caused by the particular geometry of the system and the strong magnetic fields. Laser-cooling in the current ALPHA setup will only be possible along the magnetic axis of the system and full cooling in all dimensions for both e^+ and Be^+ will require collisions. In a strong magnetic field the collisional relaxation of the axial and perpendicular (to the magnetic field) temperatures will eventually become suppressed. This effect, called magnetization, will be stronger for the e^+ than the Be^+, and while it influences the collision rates for the range of temperatures investigated in this work it remains negligible for the equilibria obtained [32, 33].

6. Antihydrogen trapping in the presence of Be^+

Due to the various heating sources we assume, as a worst case, that the sympathetic cooling must remain active during antihydrogen formation and trapping. We now consider what effects the presence of ions could have on the antihydrogen formation. We have identified two possible mechanisms by which the ions may influence antihydrogen formation and trapping: (a)

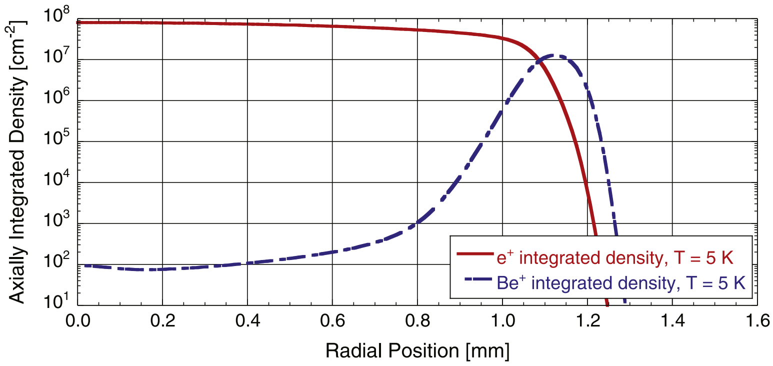

Figure 8. Axially integrated radial profiles calculated for 10^5 $^9Be^+$ ions and 2×10^6 e^+ at 5 K.

antiproton capture by Be^+ ions before antihydrogen formation and (b) ionization or annihilation of weakly bound $\bar{H}$ in collisions with Be^+ ions.

We saw earlier how the separation of the ions and positrons led to reduced cooling. However, it may serve to prevent antiproton capture by the ions. As indicated in [2] the radius of the injected antiproton cloud is usually kept at about half the positron plasma radius in order to ensure good overlap and reduce the effects the plasma rotation on the nascent $\bar{H}$. From the above equilibrium calculations shown in figure 2 we can extract the axially integrated radial profile of the ions. The combined plasma is about 2 cm long in the chosen wells, though the ions tend to concentrate in a band around the middle stretch for a slightly shorter length.

6.1. Antiproton capture by Be$^+$

Figure 8 shows the axially integrated particle density for Be^+ and e^+ at 5 K. The Be^+ integrated density in the central region where the $\bar{p}$'s are injected is of order 10^2 cm^{-2}. Adapting the argument by Sakimoto [34, 35] we can estimate an upper limit for the cross-section for $\bar{p}$-capture in $\bar{p}$-Be^+ scattering. The $\bar{p}$ capture reaction goes as

$$\bar{p} + Be^+ \rightarrow \bar{p}Be^{2+} + e^-, \tag{5}$$

where the shedding of an electron stabilizes the $\bar{p}Be^{2+}$ energetically against dissociation of the antiproton (though additional electrons can still be emitted). In the adiabatic approximation the relative angular momentum J between the $\bar{p}$ and the ion in the initial channel is conserved in the $\bar{p}Be^{2+}$ compound (i.e. no angular momentum is transferred to the electrons). Still in the adiabatic picture, the final $\bar{p}Be^{2+}$ state is a bound state in the $\bar{p}$-Be^{2+} potential. The adiabatic approximation can be expected to work particularly well in the long range, where the effective $\bar{p}$-ion interaction takes the form (expressed in atomic units)

$$V_{\rm eff}(R) = \frac{J(J+1)}{2\mu R^2} - \frac{2}{R} + E_{\rm Be^{2+}}. \tag{6}$$

Here μ is the $\bar{p}$-Be^{2+} reduced mass and $E_{Be^{2+}}$ is the energy of the Be^{2+} ion. This potential has a minimum, i.e. admits bound states, located at $R_0 = J(J+1)/(2\mu)$, with the value $V_{eff}(R_0) = -2\mu/(J(J+1)) + E_{Be^{2+}}$.

In the limit of zero collision energy E, a bound state can be formed at this minimum only if it lies below the energy in the initial channel, i.e. the energy of the Be^+ ion E_{Be^+}. Hence, we get the requirement

$$-\frac{2\mu}{J(J+1)} < E_{Be^+} - E_{Be^{2+}} = -I_2, \tag{7}$$

where I_2 is the second ionization potential of the Be atom ($I_2 = 0.669$ atomic units). This translates into a requirement for the largest angular momentum J_c which can participate in the reaction,

$$(J_c + 1)^2 \simeq J_c(J_c + 1) = \frac{2\mu}{I_2}. \tag{8}$$

For Be^+ we find that the parameters are $J_c = 70$ and $R_0 = 1.5$. Though R_0 is not very large, the length we need to compare to is the radius of the $Be^{2+}(1s^2)$ ion, which is $\sim 1/Z = 0.25$. Equation (6) thus remains a good approximation.

The partial wave expansion of the cross-section can be written as

$$\sigma = \frac{\pi}{2\mu E}\sum_J (2J+1)P^J, \tag{9}$$

where P^J is the total probability for antiproton capture for the partial wave J. An upper limit for σ can be found by setting all $P^J = 1$. Summing J up to J_c this gives

$$\sigma < \frac{\pi}{2\mu E}(J_c + 1)^2 = \frac{\pi}{I_2}\frac{1}{E} = \frac{4.7}{E}. \tag{10}$$

Using this upper limit for the cross-section the collision rate per antiproton becomes

$$\lambda = \frac{5.6 \times 10^{-7}\left[n/\mathrm{cm}^{-3}\right]}{\sqrt{[E/\mathrm{Kelvin}]}}\mathrm{s}^{-1}, \tag{11}$$

where n is the density of ions. Assuming an energy $E = 5$ K (where K is used as an energy unit) and density $n = 6 \times 10^7$ cm^{-3} (figure 2), gives the rate $\lambda = 15$ s^{-1} (while in the ion cloud). However, antiprotons predominantly find themselves on axis where the average density is about 10^5 times lower (figure 8) thus rendering this rate negligible compared to the total time of the $\bar{p}/e^+$ mixing (1 s).

6.2. Interaction of Be^+ and $\bar{H}$

To address the issue of $\bar{H}$ collisions with ions we have performed semiclassical calculation for ground state $\bar{H}$ interacting with both Be^+ and Mg^+ and find that at energies below about 1 eV, they agree with the Langevin result [36, 37]. The total inelastic cross-section for $\bar{H}$ on Be^+ ions is thus given by

$$\sigma = \frac{1.38 \times 10^{-15}}{\sqrt{E/\mathrm{eV}}}\ \mathrm{cm}^2, \tag{12}$$

where E is the collision energy in the centre of mass frame, such that the collision rate becomes energy independent and equal to

$$\lambda = v\sigma n = 2 \times 10^9 n\ \mathrm{cm}^3\ \mathrm{s}^{-1}. \tag{13}$$

Figure 2 gave typical densities for 10^5 Be^+ ions of at most $4 \times 10^7\ \mathrm{cm}^{-3}$, resulting in $\lambda = 0.08\ \mathrm{s}^{-1}$ for $\bar{\mathrm{H}}$ in the Be^+ ion region. This means a worst case survival time of 10 s. Since $\bar{\mathrm{H}}$ spend only a small fraction of their time in the centre of the trap, and the antihydrogen formation (and thus ion presence) takes only 1 s [4], these collisions are negligible.

7. Conclusions

We have presented a novel technique for enhanced antihydrogen trapping for precision experiments with cold antihydrogen. The technique expands on demonstration experiments at NIST from the turn of the century using laser-cooled ions to sympathetically cool the positron plasma used in several antihydrogen experiments. Using the example of the ALPHA experiment, we found that lighter ions are more effective due to the combined effect of centrifugal separation and improved single-collision momentum exchange. We also found, somewhat surprisingly, that increasing the number of ions beyond about 10% of the number of positrons result in diminishing returns with respect to the minimum positron temperatures achievable. We attributed this effect to the centrifugal separation that places the additional ions on the outside, too far from the positrons to supply additional cooling. We found that we could, with realistic environmental constraints, reduce the positron temperature by about an order of magnitude using laser-cooled Be^+. The ultimate temperature limit of the technique will be determined by the heating caused by the magnetic trap for the antiatoms, which must be energized before antihydrogen is formed. All other sources of heat can, in principle, be made negligible.

Due to the various heating sources the sympathetic cooling must remain active during antihydrogen formation and trapping. For this reason we also investigated how the presence of Be^+ ions could influence antihydrogen formation and trapping. We found that the centrifugal separation of Be^+ and e^+ meant that $\bar{\mathrm{p}}$ capture by Be^+ ions was a negligible effect. We also found that the cross-section for $\bar{\mathrm{H}}$ loss through collisions with Be^+ ions was negligible for typical circumstances.

In conclusion we expect that this technique should be able to significantly enhance the amount of trapped antihydrogen that will be available for experiments and thus further open the door to precision studies of antihydrogen. As our calculations of equilibrium temperatures did not take collective effects into account it is likely that once realized experimentally lower temperatures, and therefore better conditions, would ensue.

Acknowledgments

This work was supported by VR (Sweden), The Royal Society, EPSRC (UK) and NSF (USA).

References

[1] Andresen G B *et al* 2010 *Nature* **468** 673–6
[2] Andresen G B *et al* 2011 *Nat. Phys.* **7** 558–64
[3] Gabrielse G *et al* (ATRAP Collaboration) 2012 *Phys. Rev. Lett.* **108** 113002
[4] Amole C *et al* 2012 *Nature* **483** 439–43
[5] Charman A E (ALPHA Collaboration) 2013 *Nat. Commun.* **4** 1785
[6] Donnan P H, Fujiwara M C and Robicheaux F 2013 *J. Phys. B: At. Mol. Opt. Phys.* **46** 025302
[7] Andresen G B *et al* 2011 *Phys. Rev. Lett.* **106** 025002
[8] Madsen N *et al* 2005 *Phys. Rev. Lett.* **94** 033403
[9] Hurt J L, Carpenter P T, Taylor C L and Robicheaux F 2008 *J. Phys. B: At. Mol. Opt. Phys.* **41** 165206
[10] Fajans J, Bertsche W, Burke K, Chapman S F and van der W D P 2005 *Phys. Rev. Lett.* **95** 155001
[11] Bertsche W *et al* 2006 *Nucl. Instrum. Methods Phys. Res.* A **566** 746–56
[12] Andresen G B *et al* 2010 *Phys. Rev. Lett.* **105** 013003
[13] Gabrielse G *et al* (ATRAP Collaboration) 2011 *Phys. Rev. Lett.* **106** 073002
[14] Larson D J, Bergquist J C, Bollinger J J, Itano W M and Wineland D J 1986 *Phys. Rev. Lett.* **57** 70–73
[15] Myatt C J, Burt E A, Ghrist R W, Cornell E A and Wieman C E 1997 *Phys. Rev. Lett.* **78** 586–9
[16] Doyle J, Friedrich B, Krems R and Masnou-Seeuws F 2004 *Eur. Phys. J.* D **31** 149–64
[17] Jelenković B M, Newbury A S, Bollinger J J, Mitchell T B and Itano W M 2002 *Nucl. Instrum. Methods Phys. Res.* B **192** 117–27
[18] Jelenković B M, Newbury A S, Bollinger J J, Itano W M and Mitchell T B 2003 *Phys. Rev.* A **67** 063406
[19] Andresen G B *et al* 2010 *Phys. Lett.* B **685** 141–5
[20] Meerson B and Friedland L 1990 *Phys. Rev.* A **41** 5233–6
[21] Fajans J and Friedland L 2001 *Am. J. Phys.* **69** 1096–102
[22] Amole C *et al* (ALPHA collaboration) 2013 *Phys. Plasmas* **20** 043510
[23] Andelkovic Z, Cazan R, Nörtershäuser W, Bharadia S, Segal D M, Thompson R C, Jöhren R, Vollbrecht J, Hannen V and Vogel M 2013 *Phys. Rev.* A **87** 033423
[24] Phillips W D, Gould P L and Lett P D 1988 *Science* **239** 877–83
[25] Madsen N, Bowe P, Drewsen M, Hornekær L H, Kjærgaard N, Labrador A, Nielsen J S, Schiffer J P, Shi P and Hangst J S 1999 *Phys. Rev. Lett.* **83** 4301–4
[26] O'Neil T M 1981 *Phys. Fluids* **24** 1447–51
[27] Andresen G B *et al* (ALPHA Collaboration) 2011 *Phys. Rev. Lett.* **106** 145001
[28] Andresen G *et al* 2007 *Phys. Rev. Lett.* **98** 023402
[29] Funakoshi R *et al* 2007 *Phys. Rev.* A **76** 012713
[30] Fajans J, Madsen N and Robicheaux F 2008 *Phys. Plasmas* **15** 032108
[31] Madsen N (The Alpha Collaboration) 2013 *J. Phys.: Conf. Ser.* **443** 012005
[32] Beck B R, Fajans J and Malmberg J H 1996 *Phys. Plasmas* **3** 1250–8
[33] Anderegg F, Dubin D H E, O'Neil T M and Driscoll C F 2009 *Phys. Rev. Lett.* **102** 185001
[34] Sakimoto K 2006 *Phys. Rev.* A **74** 022709
[35] Sakimoto K 2010 *Phys. Rev.* A **82** 012501
[36] Langevin M P 1905 *Ann. Chim. Phys.* **T5** 245–88
[37] Gioumousis G and Stevenson D P 1958 *J. Chem. Phys.* **29** 294–9